



Dissolution Prediction of Fumaric Acid Crystal (Form A) in Ethanol using Molecular Dynamic Simulation

Siti Nurul'ain Yusop^{1*}, Wirani Anak Nili¹, Nornizar Anuar¹, Nik Salwani Md Azmi¹, Muhammad Fitri Othman¹, Syarifah Abd Rahim²

¹Faculty of Chemical Engineering, Universiti Teknologi MARA, 40450 Shah Alam, Selangor

²Faculty of Chemical and Natural Resources Engineering, Universiti Malaysia Pahang, 26600 Pekan, Pahang

*Corresponding author E-mail: sitinurul'ain@salam.uitm.edu.my

Abstract

Molecular dynamic simulation allows a better understanding on the dissolution behaviour of crystal in solvent. In this study, a dicarboxylic acid, fumaric acid crystal (Form A) is studied in ethanol which act as solvent. The morphology of fumaric acid (Form A) was successfully predicted, and the simulated lattice energy was compared with the experimental data and microphotograph of fumaric acid. The morphology was predicted using the CVFF forcefield and the lattice energy simulated was -32.8 kcal/mol, and 4.1% deviated from the experimental lattice energy. The elongated prismatic-like shape predicted morphology was in a good agreement with the microphotograph experimental fumaric acid. Ten morphological important facets were produced; (011), (020), (100), (110), (11-1) and their multiplicity. The mean square displacement (MSD) analysis through the diffusion coefficient showed that the diffusion of molecules from the crystal facets were from the following order: (11-1) > (100) > (110) > (011) > (020), which suggested the order of detachment of molecules from the respective facets. These findings were in agreement with the detachment observations carried out at 20ps of simulation, and also with the results of attachment energies, which corresponded to the growth rate of the facets and the molecular arrangement on the facets. Meanwhile, the radial distribution function on four facets showed that the molecular interactions due to van der Waals and Coulombic charges were detected in the following order: (11-1) > (110) > (011) and (100).

Keywords: Dissolution; fumaric acid; mean square displacement; morphology; radial distribution function.

1. Introduction

The dissolution rate of drug is a major concern in pharmaceutical industry, due to the dependency of drug effectiveness on its dissolution ability. Some pharmaceutical drugs have low dissolution rate and takes longer time to be consumed in human body. One of the methods to overcome the problem is by co-crystallization.

Fumaric acid is an excellent candidate as a conformer for co-crystallization process as the carboxyl group in its molecules prepares the sites for supramolecular homo-synthon and hetero-synthon interactions. Supramolecular homo-synthon such as in fumaric acid crystal composed of identical, self-complementary functionalities and dominate in the presence of single functional group [1,2]. Among the success story of fumaric acid as co-former are with an active pharmaceutical ingredient (API), ketoconazole [3], antiviral drug acyclovir [4] and carbamazepine [5]. Other commonly used co-formers to produce co-crystals with API are succinic acid, nicotinamide, salicylic acid, adipic acid, fumaric acid and succinic acid [6]. Molecular dynamic simulation is commonly used by several researchers to elucidate the molecular interactions in the crystallisation, for example, the stability study of polymorphic form of para-amino benzoic acid [7]. Molecular dynamic simulation has also been used to investigate the effect of nanostructured materials on amorphous drug and its stability [8]. The fundamental of morphology lies in the determination of the

total energies such as hydrogen bond, van der Waals and Coulombic energy as well as the crystal lattice energy. Attachment energy method is commonly used by many previous researchers [9,10,11] in prediction of crystal morphology. The lattice energy, which is a summation of attachment energy and slice energy was compared with the experimental data to confirm the validity of the predicted morphology. Dynamic simulation to evaluate the interactions between molecules are commonly assessed using radial distribution function (RDF) [12] and mean square displacement (MSD). MSD shows the distance travelled by a molecule in the system, hence giving a picture on the activity of the molecule in the system [13], meanwhile RDF describes the distance of a given particle from a reference particle by the types of bonding exists between particles.

In this work, the simulation on the prediction of fumaric acid behaviour, as one of the potential co-former was explored, with the intention to establish method of determining dissolubility of facets of the tested fumaric acid, which contain dicarboxylic acid in its molecular structure. Ethanol was used as a solvent, in the assessment for interaction between the facets molecules and solvent molecules, which aids the dissolution process.

2. Material and Methodology

2.1. Crystal Structure of Fumaric Acid (Form A Polymorph)

The fumaric acid (Form A) data file was retrieved from the Cambridge Structural Database (CSD), ref. code FUMAAC. Form A polymorph fumaric acid crystallizes in monoclinic crystal lattice with a space group P21/c and cell parameters; $a = 7.619$, $b = 15.014$, $c = 6.686$, $\alpha = 90^\circ$, $\beta = 112^\circ$ and $\gamma = 90^\circ$. Fig. 1 shows the molecular structure of fumaric acid (form A) in x-, y-, and z-directions. One unit cell of fumaric acid comprises of 14 molecules in a unit cell.

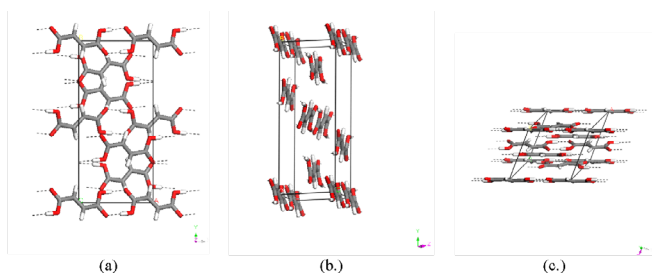


Fig. 1: (a) Molecular structure of fumaric acid (form A) in z-direction (b), x-direction (c.) and y-direction.

2.2. Morphology Prediction of Fumaric Acid (Form A)

The prediction of morphology of fumaric acid crystal was carried out using Material Studio 4.4. There were four major steps involved in the morphology prediction which are; (1) assigning the charges to the atoms, (2) optimization process to stabilize the energy of the molecule, (3) second optimization to minimize the energy of the molecule, and (4) the morphology prediction. Three methods were used to determine the charges of each atom of the fumaric acid (Form A) molecules which are MOPAC (AM1, MNDO and PM3), DMol3 (Mulliken, Hirshfeld and ESP) and the charges assigned by the forcefield itself (COMPASS, CVFF and PCFF). The crystal structure with different types of charges underwent the first optimization process, whereby the conformation of the crystal structure was kept rigid. The forcefields (COMPASS, Dreiding, Universal, CVFF and PCFF) were tested one by one on the structures. Then, the second optimization process minimized the conformation of the structures by relaxing the molecules and the same forcefield was used as the first optimization process. Then, the morphology was predicted using the same forcefield and charges as used in both optimization processes. Various forcefields were used in this work, with the intention to explore the diverse possibility of fumaric acid morphology formed using this method. The morphology prediction of fumaric acid crystal (form A) was done based on attachment energy model, which can be computed using Eq. 1.

$$E_{att} = E_{latt} - E_{sl} \quad (1)$$

where E_{att} is the attachment energy released during the growth of crystal surface, E_{latt} is lattice energy while E_{sl} is slice energy which is the energy of growth slice of a thickness, d_{hkl} or d -spacing [7]. The crystal surfaces' growth rate, R_{hkl} is proportional to the absolute attachment energy [13].

$$R_{hkl} \propto |E_{att}| \quad (2)$$

This imply that the lower the E_{att} , the slower the growth rate at that crystal surface.

2.2. Dissolution of Fumaric Acid (Form A) in Ethanol Solvent

The dissolution prediction of fumaric acid also was carried out using the embedded module in Material Studio version 4.4. The solvent, ethanol was constructed in a periodic amorphous a cell using 5,000 number of molecules, which to be interacted with a fumaric acid crystal. The ethanol molecules at center of the amorphous cell were removed and the ethanol at the edges of the of the ethanol cell was set to be at a rigid state, leaving only 2,000 ethanol molecules ready to be interacted with the crystal morphology. A fumaric crystal was later inserted at the center of the amorphous cell. The cell containing ethanol molecules and a fumaric crystal was optimized using CVFF forcefield and Ewald summation method. Next, the optimized molecules were set for dynamic simulation procedure using the same combination of forcefield and summation method. The total simulation time was 20ps, with 1fs time step. The temperature was controlled using Berendsen thermostat and NVT (constant number of molecules, constant volume and constant temperature) ensemble. The trajectory of the data was recorded every 1000 ps and successful dynamic simulation data was analyzed using mean square distribution (MSD) and radial distribution function (RDF).

A diffusion coefficient was determined from the slope of MSD vs time graph. Diffusion coefficient, D was calculated from the Einstein relation as depicted in Eq. 3. The $r_i(t)$ and $r_i(0)$ is the coordinates of particle i at time t and initial time, respectively; while $\langle [r_i(t) - r_i(0)]^2 \rangle$ is the mean square displacement (MSD) of coordinates [15]:

$$D = \frac{1}{6} \lim_{t \rightarrow \infty} \frac{d}{dt} \sum_{i=1}^N \langle |r_i(t) - r_i(0)|^2 \rangle \quad (3)$$

3. Results and Discussion

3.1. Morphology Prediction of Fumaric Acid (Form A)

Table 1 shows the values of computed lattice energies of fumaric acid (form A) using different forcefields and charges. The difference between experimental lattice energy and simulated lattice energy was also recorded in this work. The experimental lattice energy for fumaric acid is -31.5 kcal/mol [17]. The percents difference between the values ranges between 2.6% and to 355.4%. The predicted morphology chosen from this work is based on % difference of less than 5%, and the predicted morphology must resemble the microphotograph of crystal grown during the experiment. According to Table 1, none of the morphology predicted using atom charge-assigned by using MOPAC and DMol3 gave less than 5% percentage difference. Meanwhile, for atom charge-assigned by forcefield, some shows less than 5% difference from the experimental value, such as the data optimized and predicted morphology using forcefield such COMPASS, and CVFF. Although COMPASS forcefield shows the lowest percentage difference (2.6%), the morphology predicted was not in agreement with the microphotograph. Meanwhile, the data obtained using CVFF forcefield shows the second lowest percentage error (4.1%) and the morphology predicted was in elongated prismatic-like shape, which resembles the morphology from the experimental data [16]. Therefore, the morphology with CVFF forcefield was chosen in this study for dissolution study in the presence of ethanol. The comparison of the predicted fumaric acid (Form A) and the experimental morphology is shown in Fig. 2, in which the morphology produced is an elongated prismatic shape. It can be seen that the predicted fumaric acid morphology has ten important facets, which are (020), (011), (100), (110) and (11-1) with their multiplicities, as shown in Table 2. Facet (020) is the largest

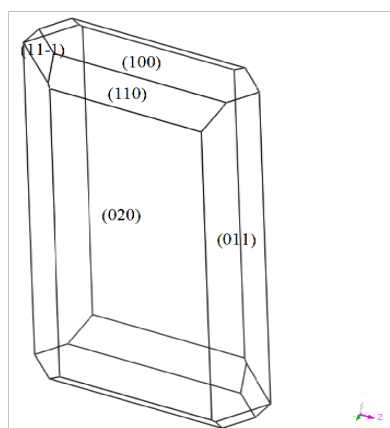
surface making them the dominant face, which indicates the slowest growth and the most morphological important facet [18,19].

there is no O-H connection at the end of exposed fumaric acid molecule as present in facet (020). All the exposed H and OH of the molecules are the sites for hydrogen bonding between fumaric

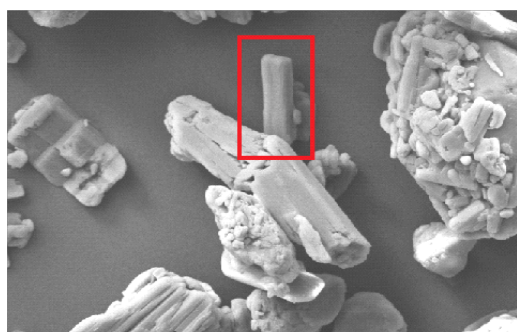
Table 1: Computed lattice energies of fumaric acid and its percentage error

CHARGE TYPE	Forcefield									
	COMPASS		Dreiding		Universal		CVFF		PCFF	
	E_{latt}	(%) ^a								
AM1	-55.3	75.6	-97.1	208.2	-33.8	7.3	-41.4	31.3	-44.5	41.4
MNDO	-51.8	64.4	-87.6	178.2	-35.7	13.4	-37.1	17.6	-44.4	40.9
PM3	-56.4	79.2	-92.1	192.2	-37.7	19.8	-39.1	24.1	-45.9	45.8
MULLIKEN	-84.3	167.8	-136.9	334.74	-43.5	38.1	-48.1	52.6	-58.4	85.4
HIRSHFELD	-35.9	14.0	-68.6	117.8	-29.5	6.43	-34.5	9.64	-41.2	30.9
ESP	-103.5	228.4	-143.4	355.4	-48.1	52.6	-54.3	72.3	-60.5	92.2
COMPASS	-32.3	2.6	-	-	-	-	-	-	-	-
CVFF	-	-	-	-	-	-	-32.8	4.1	-	-
PCFF	-	-	-	-	-	-	-	-	-45.7	45.0

^aExperimental lattice energy used was -31.5 kcal/mol [10]



(a)



(b)

Fig. 2: (a) Morphology of fumaric acid (Form A) from Material Studio (b.) Microphotograph of fumaric acid [16].

Fig. 3 shows the molecular arrangement of each facet. The molecules are found, to be homosynthon which composed of identical functionality, dominated by O-H-O connection between the molecules. Facet (011) has considerably smooth surface as compared to 4 other facets. Facet (020) has a rough surface with upper half of the molecule structure exposed. Meanwhile, facet (100), (110) and (11-1) have a rough, non-uniform surface with half of a fumaric acid (form A) molecule are exposed. In facet (020), the fumaric acid molecules are bonded together with O-H-O connection with the end part of fumaric acid molecule exposed with O-H readily exposed from the facet. The facet (100), (100) and (11-1) have half exposed fumaric acid molecules. However,

acid and the foreign molecules. Table 2 shows the attachment and slice energies of each facet, and the surface with the lowest attachment energy has the largest surface area [20].

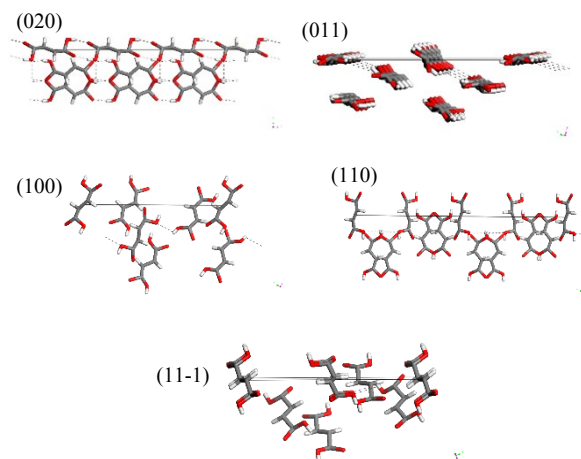


Fig. 3: Surface of each facet of Fumaric Acid form A

Table 2: Multiplicity, d-spacing, attachment and slice energies of fumaric acid morphology facets.

Face	Multiplicity	d-spacing	Attachment energy (kcal/mol)	Slice energy (kcal/mol)
(020)	2	7.49	-10.23	-22.57
(011)	4	5.96	-11.35	-21.45
(100)	2	7.70	-18.17	-14.63
(110)	4	6.85	-18.79	-14.01
(11-1)	4	5.42	-21.72	-11.08

From Table 2, the lowest absolute attachment energy is the attachment energy of facet (020) with the value of 30.68 kcal/mol. Theoretically, this facet (020) is the slowest surface growth, hence making it the most morphologically important facet. Facet (020) with the lowest attachment energy (-10.23 kcal/mol), comprises of -1.05 kcal/mol of electrostatic charge and -9.12 kcal/mol of van der Waals forces, is the largest surface with area (29.5%). The second facet with the lowest attachment energy is facet (011) with value of -11.35 kcal/mol followed by facet (100) and (110) with attachment energy of -18.17 kcal/mol and -18.79 kcal/mol respectively. Meanwhile, facet (11-1) has the largest absolute attachment energy of -21.72 kcal/mol with 2.2% total surface area.

3.2. Dissolution of Fumaric Acid (Form A) in Ethanol Solvent

Fig. 4 shows the result of dynamic simulation, in which the total simulation time was 20ps. At 20ps, the fumaric acid molecule was observed detached from the crystal habit and partially lost its shape, especially for facets at the corner edge (11-1). This then is followed by the smaller facets (100) and (110) and the rest of the facets (011) and (020). This observation also was supported by the mean square displacement (MSD) analysis of a successful dynamic simulation, as shown in Fig. 6. The diffusion coefficient, D of the crystal surface was calculated from the slope of the MSD lines (Fig. 6) and the Einstein equation (Eq. 3).

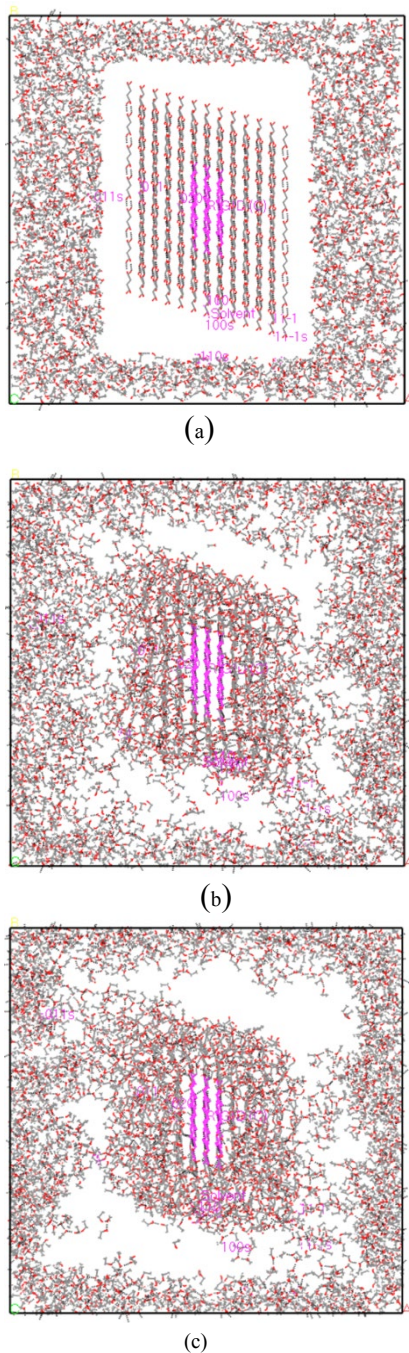


Fig. 4: (a) before (0ps) simulation time, (b) at 10 ps simulation time, (c) at 20 ps simulation time

Interpretation of MSD lines in Fig. 5 shows that the smallest facet (11-1) has the highest diffusivity coefficient, D . The rank of the diffusion coefficient is as follow;

1. (11-1) $0.6889 \text{ \AA}^2/\text{ps}$
2. (100) $0.4030 \text{ \AA}^2/\text{ps}$
3. (110) $0.2131 \text{ \AA}^2/\text{ps}$
4. (011) $0.1509 \text{ \AA}^2/\text{ps}$
5. (020) $0.0794 \text{ \AA}^2/\text{ps}$

The higher displacement (and hence higher diffusion coefficient) indicates a stronger movement of molecules and vice versa [21]. Facet (020) proves to be the slowest surface to be diffused with the lowest number of $0.0794 \text{ \AA}^2/\text{ps}$ and facet (11-1) was the fastest surface to be diffused to the surrounding area. The MSD curve and

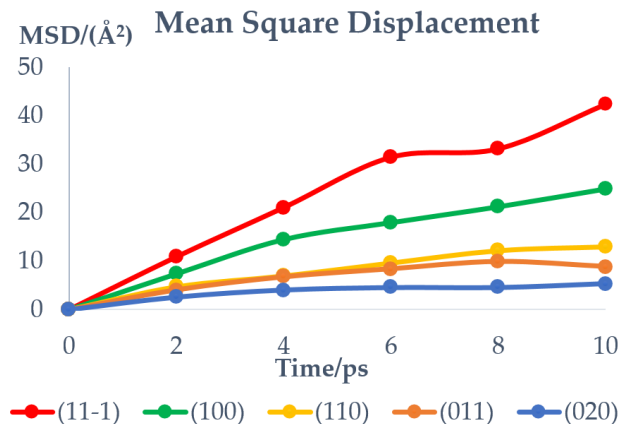


Fig. 5: MSD fumaric acid in ethanol solvent

calculated values of diffusion coefficient values supported the morphology observation (Fig. 1a) and the result tabulated in Table 2. Fig. 6 shows the radial distribution function (RDF) of fumaric acid for four different facets; (001), (100), (110) and (11-1). The peak at lower than 3.5 \AA indicates the contribution of hydrogen bonding while the peak higher than 3.5 \AA is mainly consists of Coulomb and van der Waals forces [13]. From Fig. 6, it shows that the peaks of all facets are between 16 to 34 \AA which indicate that the main interactions exist are van der Waals and Coloumbic forces only.

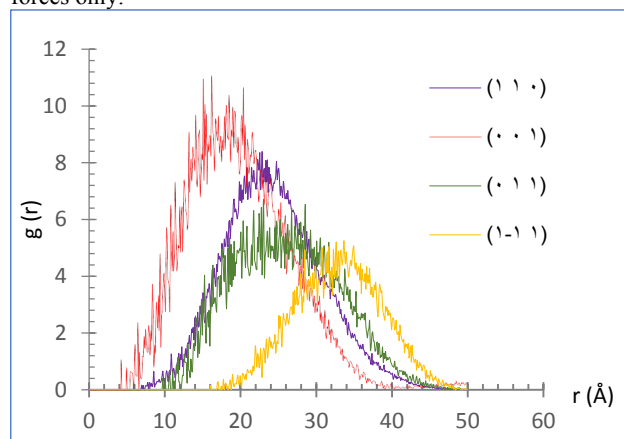


Fig. 6: RDF for fumaric acid (form A) in ethanol solvent

4. Conclusion

In conclusion, this study has successfully predicted the morphology of fumaric acid crystal (form A), i.e. an elongated prismatic shape using the CVFF forcefield. Ten morphological important facets were (011), (020), (100), (110), (11-1) and their multiplicity. The most morphologically important facets base on the attachment energy values were found to be (020), (011), (100),

(110) and (11-1). The mean square displacement (MSD) analysis through the diffusion coefficient showed that the diffusion of molecules from the crystal facets were from the following order: (11-1) > (100) > (110) > (011) > (020), which suggested the order of detachment of molecules from the respective facets. These diffusion orders were in an agreement with the detachment observation of the molecules carried out at 20ps simulation time ((11-1) > (100) > (110) > (011) > (020)). These results also corresponded well to the results of attachment energies and facets areas obtained from morphology prediction work, as well as the molecular arrangement on the facets. Meanwhile, the radial distribution function on four facets showed that the molecular interactions due to van der Waals and Coulombic charges were detected in the following order: (11-1) > (110) > (011) and (100).

Acknowledgement

The authors would like to express their gratitude to the Ministry of Higher Education, Malaysia for funding this work, which was carried out at Faculty of Chemical Engineering, Universiti Teknologi MARA. This work was funded by the research grant 600-RMI/MyRA 5/3/BESTARI (023/2017) and (600-IRMI/MyRA 5/3/GIP(066/2017)).

References

- Aakeroy, C. B., Desper, J., Helfrich, B. A., "Heteromeric intermolecular interactions as synthetic tools for the formation of binary co-crystals," *Cryst. Eng. Comm.*, vol. 6, no. 5, pp. 19-24, 2004.
- Adalder, T. K., Sankolli, R., Dastidar, P., "Homo- or heterosynthon? A crystallographic study on a series of new cocrystals derived from pyrazinecarboxamide and various carboxylic acids equipped with additional hydrogen bonding sites." *Crystal Growth & Design*, vol. 12, no. 5, pp. 2533-2542, 2012.
- Martin, F. A., Pop, M. M., Borodi, G., Filip, X., Kacso, I., "Ketoconazole salt and co-crystals with enhanced aqueous solubility," *Cryst. Growth Des.*, vol. 13, no. 10, pp. 4295-4304, 2013.
- Sarkar, A., Rohani, S., "Cocrystal of Acyclovir with promising physicochemical properties," *J. Pharm. Sci.*, vol. 104, pp. 98-105, 2015.
- Rahim, S.A., Rahman, F.A., Nasir, E.N.E.M., Ramle N.A., "Carbamazepine co-crystal screening with dicarboxylic acids co-crystal formers," *Int. J. Chem. Mol. Eng.*, vol. 9, no.5, pp. 442-445, 2015.
- Rahman, F.A., Rahman, S.A., Tan, C.C., Low, S.H., Ramle, N.A., "Carbamazepine-Fumaric Acid and Carbamazepine-Succinic Acid Co-crystal Screening Using Solution Based Method," *Int. J. Chem. Eng. Appl.*, vol. 8, no. 2, pp. 136-140, 2017.
- Toroz, D., Hammond, R. B., Roberts, K. J., Harris, S., Ridley, T., "Molecular dynamics simulations of organic crystal dissolution: The lifetime and stability of the polymorphic forms of para-amino benzoic acid in aqueous environment." *J. Cryst. Growth*, vol. 401, pp. 38-43, 2014.
- Yani, Y., Chow, P. S., Tan, R. B., "Pore size effect on the stabilization of amorphous drug in a mesoporous material: Insights from molecular simulation," *Microporous Mesoporous Mater*, vol. 221, pp. 117-12, 2016.
- Zhang, Y., "Prediction and Theoretical Investigation of the Morphology of Erythromycin Dihydrate Crystals," *Trop. J. Pharm. Res.*, vol. 13, no. 6, pp. 829-834, 2014.
- Rosbottom, I., Roberts, K.J., Docherty, R., "The solid state, surface and morphological properties of *p*-aminobenzoic acid in terms of the strength and directionality of its intermolecular synthons," *Cryst. Eng. Comm.*, vol. 17, pp. 5768-5788, 2015.
- Hammond, R.B., Ramachandran, V., Roberts, K.J., "Molecular modelling of the incorporation of habit modifying additives: α -glycine in the presence of L-alanine," *Cryst. Eng. Comm.*, vol. 13, pp. 4935-4944, 2011.
- Concu, R., Natalia, M., Cordeiro, D.S., "Molecular Dynamics Simulation Study of the Selectivity of a Silica Polymer for Ibuprofen," *Int. J. Mol. Sci.*, vol. 1083, pp. 1-11, 2016.
- Shi, W., Xia, M., Lei, W., Wang, F., "Solvent effect on the crystal morphology of 2, 6-diamino-3, 5-dinitropyridine-1-oxide: A molecular dynamics simulation study," *J. Mol. Graphics Modell.*, vol. 50, pp. 71-77, 2014.
- Berkovitch-Yellin, Z., "Toward an ab initio derivation of crystal morphology," *J. Am. Chem. Soc.*, vol. 107, no. 26, pp. 8239-8253, 1985.
- Rao, Z., Zheng, C., Gen, F., "Proton conduction of fuel cell polymer membranes: Molecular dynamics simulation," *Comput. Mater. Sci.*, vol. 142, pp. 122 - 128, 2018.
- Bruni, G., Maietta, M., Maggi, L., Bini, M., Capsoni, D., Ferrari, S., Marini, A., "Perphenazine-fumaric acid salts with improved solubility: preparation, physico-chemical characterization and in vitro dissolution," *Cryst. Eng. Comm.*, vol. 14, no. 18, 6035-6044, 2012.
- Derissen, J. L., Smit, P. H., "Intermolecular interactions in crystals of carboxylic acids. IV. Empirical interatomic potential functions," *Acta Crystallogr., Sect. A: Cryst. Phys., Diffr., Theor. Gen. Crystallogr.*, vol. 34, no. 6, pp. 842-853, 1978.
- Clydesdale, G., Roberts, K.J., Telfer, G.B., Grant, D.J.W., "Modelling the Crystal Morphology of α -Lactose Monohydrate," *J. Pharm. Sci.*, vol. 86, pp. 135-141, 1997.
- Schmidt, C., Yürüdü, C., Wachsmuth, A., Ulrich, J., "Modeling the Morphology of Benzoic Acid Crystals Grown from Aqueous Solution," *Cryst. Eng. Comm.*, 13, 1159-1169, 2011.
- Anuar, N., Wan Daud, W. R., Roberts, K. J., Kamarudin, S. K., Tasirin, S. M., "Morphology and associated surface chemistry of L-isoleucine crystals modeled under the influence of L-leucine additive molecules." *Cryst. Growth Des.*, vol. 12 no. 5, pp. 2195-2203, 2012.
- Ghiozizadeh, R., Wang, Y., Yu, Y.X., "Molecular dynamic simulations of stability at the early stages." *J. Mol. Struct.*, vol. 1138, pp. 198-200, 2017.